Corrosion Science 103 (2016) 66–74

Contents lists available at ScienceDirect

Corrosion Science

journal homepage: www.elsevier.com/locate/corsci

Electrochemical study the corrosion behaviour of carbon steel in mortars under compressive and tensile stresses

Xingguo Feng [a,*], Xiangyu Lu [b], Yu Zuo [c], Ning Zhuang [a], Da Chen [a,*]

[a] Jiangsu Key Laboratory of Coast Ocean Resources Development and Environment Security, Hohai University, Nanjing 210098, Jiangsu, China
[b] School of Materials Science and Engineering, Jiangsu University of Science and Technology, Zhenjiang 212003, Jiangsu, China
[c] School of Materials Science and Engineering, Beijing University of Chemical Technology, Beijing 100029, China

ARTICLE INFO

Article history:
Received 24 March 2015
Received in revised form 4 November 2015
Accepted 5 November 2015
Available online 10 November 2015

Keywords:
A. Concrete
A. Steel reinforced concrete
B. Polarization
B. EIS
C. Interfaces

ABSTRACT

The influence of compressive and tensile stresses on the corrosion behaviour of the rebar in mortars was investigated. The corrosion of the rebar intensified with increasing magnitude of the stress. Results of electrochemical impedance spectroscopy and the observed corrosion state indicated that the stress-induced corrosion of the rebar resulted mainly from degradation of the concrete/rebar interface. For the same magnitude of stress, the rebar in the compressed sample was more severely corroded than that in the tensile sample. In addition, modes were proposed to illustrate the different failure patterns of the concrete/rebar interface, owing to the action of the stresses.

1. Introduction

The durability of concrete structures is reduced primarily by the corrosion of steel bars [1]. In practice, engineering structures are subjected to various types of loading or stress and as such, many researchers have evaluated the effect of loads on the durability of the concrete structure. Anhvu [2] studied the corrosion behaviour of steel wires under tensile stresses and found that pitting corrosion attacks evolved into stress corrosion cracking. Furthermore, the corrosion led to a severe decrease in the ultimate strain, thereby resulting in brittle failure of the corroded wire. Jaffer [3] examined the distribution of corrosion products of steel rebar and found that, compared to static loading, dynamic loading resulted in a greater detachment of bonds between the aggregate and the cement paste. Moreover, owing to the opening and closing of cracks under dynamic loading, corrosion products moved away from the concrete/rebar interface and into the crack of the concrete cover layer. Ahn [4] studied the corrosion behaviour of concrete beams under static and fatigue loading, respectively, in the simulation tidal zone. In that work, the beam subjected to fatigue loading deteriorated more rapidly than its statically loaded counterpart. The former also exhibited a lower ultimate strength bearing capacity than the latter at the end of the experiments. In other work, Hariche et al. [1] determined the effect of the corrosion of rebars on the serviceability of reinforced concrete beams under loading; this study revealed that the deflection of the beam increased with progressive corrosion of the reinforcement. In fact, the deflection increased significantly during the early stages of corrosion, owing to crack propagation on the tensile side of the beams. The authors attributed this increase to the flexural tension and the expansive stresses induced by the corrosion products. Valiente [5] found that the strength and ductility of the pre-stressed steel wire in a concrete line meant for water supply, decreased significantly when the concrete cover layer was not damaged. In addition, Fang et al. [6] evaluated the bond behaviour of the corroded reinforcement in a concrete structure and found that cyclic loading led to a significant reduction in the bond capacity. The results also indicated that severe corrosion will result in substantial reduction of the bond capacity under cyclic loading. Furthermore, Arteaga et al. [7] found that the coupled effect of corrosion and fatigue led to a substantial reduction in the expected lifetime of concrete structures subjected to corrosion and fatigue deterioration processes. Apostolopoulos [8] investigated the low-cycle fatigue behaviour of corroded reinforcing steel and found that the number of cycles to failure decreased significantly with increasing amount of corrosion. In addition, Blunt and Ostertag [9] compared the corrosion behaviour of rebar in control and hybrid-fiber-reinforced concrete beams under cyclic flexural loading; they found that the start of corrosion was delayed and the corrosion rate of the rebar in the latter was lower than that of its counterpart in the former. Previous stud-

* Corresponding author. Fax: +86 25 83786611.
E-mail addresses: fengxingguo@hhu.edu.cn (X. Feng), chenda@hhu.edu.cn (D. Chen).

http://dx.doi.org/10.1016/j.corsci.2015.11.006
0010-938X/

ies indicated that applied loading accelerates the degradation of concrete structures. This is especially true for structures subjected to dynamic loading [3,6] or fatigue loading [4,7,8].

The corrosion behaviour of concrete elements under compressive and tensile stresses has also been extensively investigated [10–12]. One study showed that, compared to tensile stresses of the same magnitude, compressive stresses led to more severe corrosion of the passive film on the rebar in a chloride-free cement extract (CE) solution [10]. Zhang [11] also studied the corrosion behaviour of carbon steel in a simulated concrete pore solution, under static tensile and compressive stresses; the corrosion current density of the former was found to be lower than that resulting from the action of a compressive stress in the chloride-free pore solution. However, the tensile carbon steel sample was more severely corroded than its compressed counterpart when chlorides were added to the pore solution. Aveldaño and Ortega [12] compared the degradation of tensile and compressed concrete beams; this study revealed that cracking of the cover was more extensive in the latter (but with less loss of the bars) than in the former. Previous studies [10–12] reported conflicting results about the effect of tensile or compressive stresses on the degradation of concrete structures. Therefore, the effect of these stresses on the corrosion performance of rebar in the concrete structure, is elucidated via open circuit potential (OCP), linear polarization resistance (LPR), and electrochemical impedance spectroscopy (EIS) measurements. The results indicate that, for the same magnitude of stress, the rebar in the compressed concrete samples is more severely corroded than that in the tensile samples. Moreover, modes are introduced to explain the difference in the degradation of the concrete/rebar interface under the action of tensile and compressive stresses.

2. Experimental methods

2.1. Materials

Carbon steel rods (diameter: 10 mm) were used in this study. The chemical composition of the steel was (wt.%): 0.37% C, 0.16% Si, 0.32% Mn, 0.053% S, and 0.026% P. Plain round bars were cut to a length of 190 mm and ground with emery paper up to No.600. The samples were then degreased with acetone, rinsed with alcohol, and dried in hot air. In preparation for electrochemical testing, copper wires were subsequently welded at one end of each sample. The rebar samples were then coated with epoxy resin, leaving a 50 mm × 5 mm exposed region in the middle.

After the coating solidified, each rebar was embedded in a mold and the mortar was poured into the mold. The mortar samples, having sizes as shown in Fig. 1, were mixed with ordinary Portland cement (P.O 42.5) and river sand. The granular distribution of the sand (Fig. 2) was obtained by sieving the sand through sieve sets with sizes of 1180 μm, 750 μm, 600 μm, 425 μm, 250 μm, 150 μm, and 75 μm, respectively. In addition, the sand-cementitious material ratio and water–cement ratio (W/C) of the mortar were maintained at 3 and 0.5, respectively. The samples

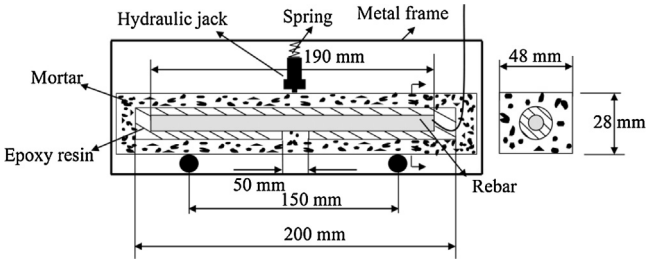

Fig. 1. Schematic of the mortar sample and loading mode.

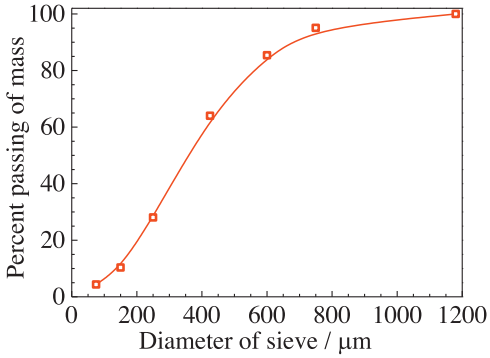

Fig. 2. The distribution of grains in the river sand.

were removed from the molds after 24 h and the surfaces of the mortar were coated with epoxy resin except for the side face of the exposed rebar. After the resin solidified, the mortars were subjected to three-point loading. The effect of stress on the corrosion behaviour of rebar in the concrete was determined by applying var-

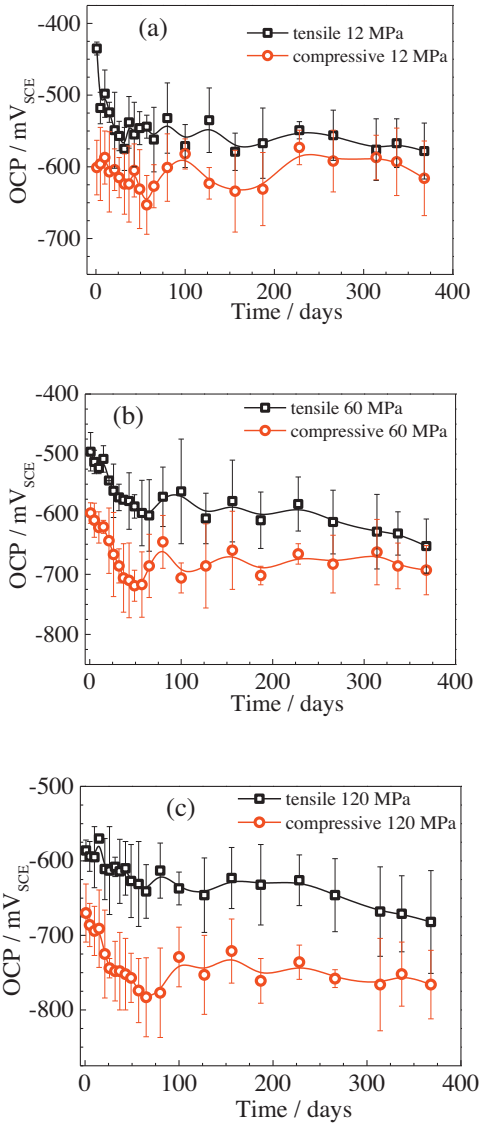

Fig. 3. OCP values of the rebar in the mortar subjected to compressive and tensile stresses of (a) 12 MPa, (b) 60 MPa, and (c) 120 MPa, while immersed in a 3% NaCl solution.

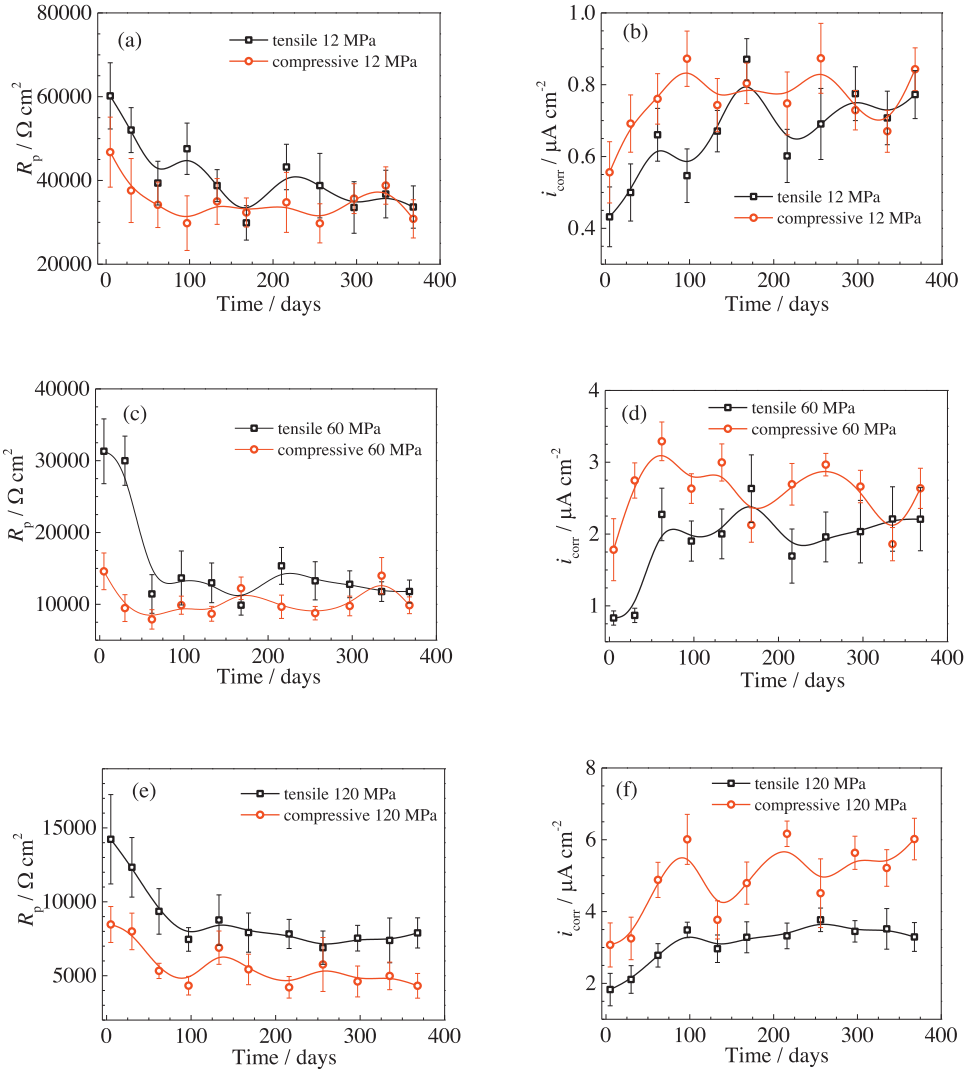

Fig. 4. Variation in R_p and i_{corr}, respectively, of the rebar in mortars subjected to stresses of (a) and (b) 12 MPa, (c) and (d) 60 MPa, and (e) and (f) 120 MPa, while immersed in a 3% NaCl solution.

ious loads; 0.5-kN-, 2.5-kN-, and 5-kN-loads (equivalent to 12 MPa, 60 MPa, and 120 MPa, respectively, tensile or compressive stresses were applied at the midpoint of the surface [13]) of the samples. The loads were applied using the apparatus shown in Fig. 1. No visible cracks were observed on the surface of the stressed mortars. The loading samples were maintained in the solutions of 3.0% (wt.%) sodium chloride. Three samples were prepared for each applied load.

2.2. Experiments

The OCP of the rebar was recorded after various immersion times; LPR and EIS measurements were also performed. The electrochemical measurements were performed at room temperature using a PARST 2273 (Princeton) instrument, with a platinum electrode and a saturated calomel electrode (SCE) as the counter and reference electrodes, respectively. In addition, the LPR measurement was performed at voltages of ±10 mV, with respect to the OCP, and a scan rate of 10 mV/min [14]. The EIS measurements were performed at frequencies ranging from $10^5 - 10^{-2}$ Hz, and the electrodes were connected and stabilized for 10 min prior to testing. During the measurements, an AC perturbation of 10 mV was applied, at the OCP, to the steel electrode. The OCP and the LPR presented in this study correspond to the average values determined from the measurements of three samples; the middle curve among the three EIS curves measured for each stress is used as the result. Moreover, the cracks formed in the mortar, at various applied loads, were examined after 357 days. The corrosion state of the rebar was examined after removing the mortar cover layers.

3. Results and discussion

3.1. Open-circuit potential

The OCP (Fig. 3) of the samples was monitored during testing. As Fig. 3 shows, the OCP of the samples decreased in the initial stage of immersion, stabilized within 50 days, and maintained values of approximately −550 mV_{SCE} to −800 mV_{SCE}, thereafter. This result is consistent with those of Dong [14], who reported that scratched-epoxy-coated rebar had a corrosion potential of approximately −700 mV_{SCE} during the stable stage. In addition, Fig. 3 shows that the OCP value of the sample subjected to compressive stresses is always more negative than that of the sample subjected to tensile stresses. Aveldaño et al. [12] investigated the corrosion behaviour of rebar in concrete beams under compression and tension, respectively, and also found that the corrosion potential of the former is

more negative than that of the latter. They attributed this to the hindrance of the movement of oxygen through the compressed concrete towards the rebar. In the present study, the OCP value decreased with increasing stress, as evidenced by values of approximately –600 mV_{SCE} and –800 mV_{SCE} at tensile stresses of 12 MPa and 120 MPa, respectively.

3.2. Linear polarization resistance

The polarization resistance (R_p) of the rebar was determined at various applied stresses and the corresponding corrosion current density (i_{corr}) was calculated from the resistance as follows:

$$i_{corr} = \frac{\beta_a \beta_c}{2.303 R_p \left(\beta_c - \beta_a\right)} \quad (1)$$

$$B = \frac{\beta_a \beta_c}{2.303 \left(\beta_c - \beta_a\right)} \quad (2)$$

$$i_{corr} = \frac{B}{R_p} \quad (3)$$

where β_a and β_c are the anodic and cathodic Tafel slopes, respectively, on a log scale [14]. Previous studies indicated that carbon steel bar in concrete has respective anodic and cathodic Tafel slopes of ~90 mV/dec and −180 mV/dec [15–17]. Therefore, the value of B = 26 mV/dec, concurs with the experimental observations for actively corroding steel in concrete [18]. As such, in the present study, the i_{corr} values were all determined from Eq. (3), using this B value [15–17]. The result (Fig. 4) shows that the corresponding Rp decreases significantly in the first 50 days and remains relatively stable thereafter. For the same level of stress, the R_p and i_{corr} of the rebar in samples under tension are higher (in general) and lower respectively, than those of the rebar in the compressed samples. This concurs with the OCP results, which indicated that the samples subjected to compressive stresses suffered more severe corrosion attack than those subjected to tensile stresses.

Moreover, the i_{corr}, which has a magnitude of several μA/cm^{-2}, increases substantially with the magnitude of the stress. Yalçyn [19] reported i_{corr} values of the same order of magnitude as that of carbon steel in chloride-containing concrete. However, the i_{corr} values determined in this study are considerably higher than that of scratched-epoxy-coated rebar embedded in chloride-free concrete in an oceanic environment [14]. The i_{corr} results indicate that the stress applied to the samples degraded the concrete covers and accelerated the corrosion of the rebar; this degradation effect increases with increasing applied stress.

3.3. Electrochemical impedance spectroscopy

The Nyquist plots of rebars in concrete subjected to various stresses, while immersed in 3.0% sodium chloride solutions are presented in Fig. 5. As the figure shows, the radius of the capacitive loop decreases significantly with increasing stress magnitude. Furthermore, the impedance value of the rebar subjected to compressive stresses is substantially lower than that of the rebar subjected to tensile stresses of the same magnitude.

The EIS results are fitted to an equivalent circuit (Fig. 6) by using the Zsimpwin software [20,21]; R_s represents the resistance of the solution, R_{con} and C_{con} are the resistance and capacitance, respectively, of the concrete cover layer, R_t is the polarization resistance, and Q is the double layer capacitance [21,22]. As Fig. 7 shows, the equivalent circuit provides an excellent fit of the experimentally measured data.

The fitted results of R_{con} and R_t are shown in Fig. 8. R_t decreases with increasing stress and the values determined via the EIS (Fig. 8(b)) are similar to those obtained from the linear polarization

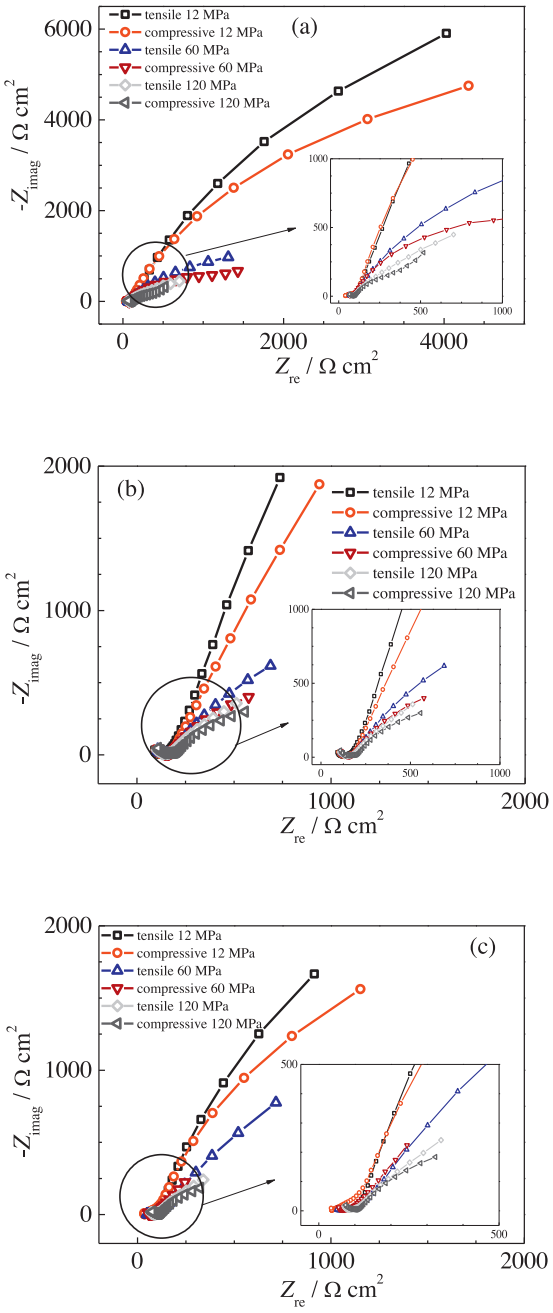

Fig. 5. Nyquist plots of the rebar in mortars subjected to various stresses for (a) 35 days, (b) 150 days, and (c) 300 days, while immersed in a 3% NaCl solution.

tests (Fig. 4). Moreover, the samples that are subjected to compressive stresses have significantly lower R_t than their counterparts that are subjected to tensile stresses. R_t (Fig. 8(b)) exhibits similar trends to those observed in the case of the OCP (Fig. 3) and the LPR (Fig. 4); this similarity further confirms that the samples

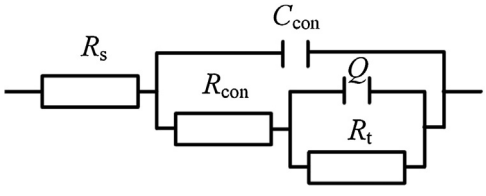

Fig. 6. Equivalent electrical circuit used for modelling of the impedance data.

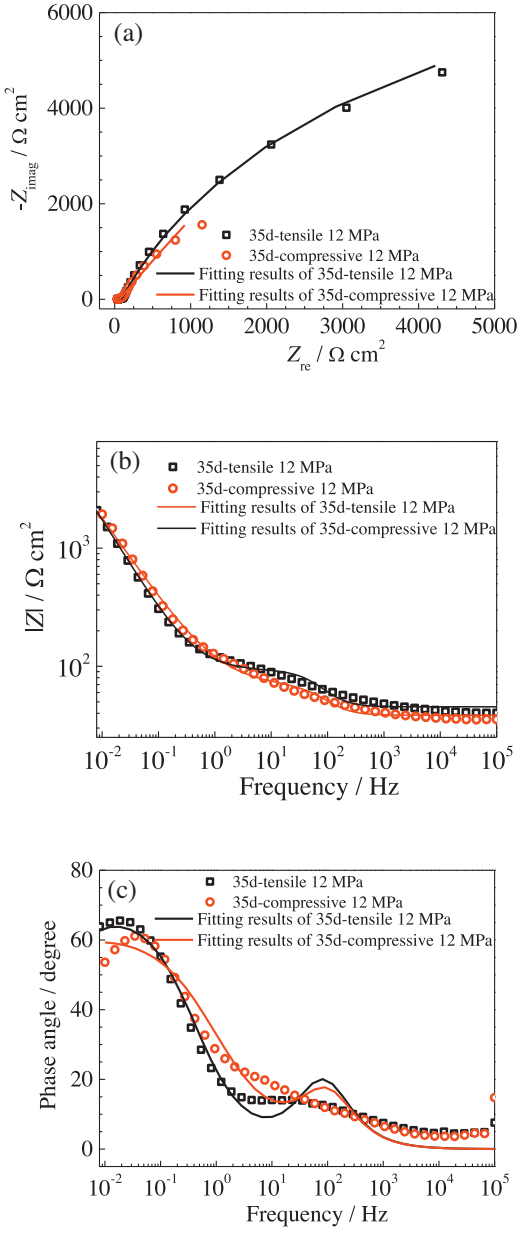

Fig. 7. The experimental and fitted EIS results of the rebar in mortars subjected to a 12 MPa stress, after being immersed in a 3% NaCl solution for 35 days.

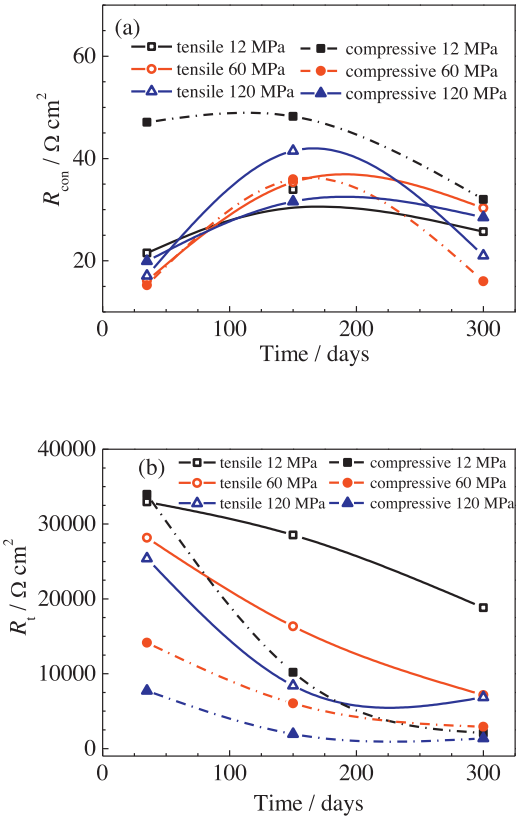

Fig. 8. Experimentally determined and fitted EIS results of the resistance of the concrete cover layer (R_{con}) and the polarization resistance (R_t) after various times, (a) R_{con}, (b) R_t.

subjected to compressive stresses are more significantly degraded than those that experience tensile stresses. R_t is, however, considerably higher than R_{con}. Morris et al. [23] conducted an EIS study of the inhibition efficiency of a migrating corrosion inhibitor, and also found that R_{con} is significantly lower than R_t. Moreover, the stress applied to the samples has a significant effect on the R_t, but has only a modest influence on the R_{con}. These results concur with those of previous studies [24–26], which suggested that the degradation of the concrete-reinforcement interface is correlated with the corrosion of the reinforcement. This suggests that the stress applied to the samples results mainly in the degradation of the concrete/steel rebar interface and hence, the applied stress accelerated the corrosion of the rebars.

3.4. Corrosion of the samples

The applied stress was removed after 357 days and the cracks in the concrete samples were examined; the morphology of the cracks is shown in Fig. 9. As the figure shows, samples subjected to a 12 MPa stress have crack-free surfaces (Fig. 9(a) and (b)). However, a longitudinal (Fig. 9(c)) and a transverse crack (Fig. 9(d)) are formed on the surface of the sample subjected to 60 MPa tensile and compressive stresses, respectively. Both longitudinal and transverse cracks formed on the surface of samples subjected to either 120-MPa tensile or compressive. These results indicate that the severity of cracking increases with increasing stress.

The corrosion of the rebar (Fig. 10) is revealed by removing the concrete. As the figure shows, the exposed regions of the rebar are all severely corroded. In the case of the sample exposed to the 12 MPa stress (Fig. 10(a) and (b)), the corrosion products formed only on the exposed region of the rebar. However, in the sample subjected to the 60 MPa stress, rust formed in both the exposed region and the vicinal zone under the epoxy resin coating (Fig. 10(c), (d)). The extent of corrosion increases when the stress is further increased to 120 MPa, and even the resin-coated region becomes severely corroded (Fig. 10(e) and (f)). These results are consistent with those (Figs. 3, 4 and 8) obtained from electrochemical testing; taken together, these results confirm that the corrosion of the rebar increases substantially with increasing magnitude of the stress. The number of cracks formed in the concrete cover layer also increases with increasing applied stress, and in turn accelerates the diffusion of aggressive ions (Cl^-) to the surface of the rebar [3,27]. Furthermore, as Fig. 8 shows, the interface of the concrete/rebar is severely degraded with increasing stress, thereby leading to a reduction in the polarization resistance. The stress distributed on the rebar also increases the activity and reduces the passivity of the rebar [28,29]. Therefore, the corrosion of the rebar increases significantly (Fig. 10) with increasing magnitude of the stress.

However, compressive stresses higher than 60 MPa result in more severe corrosion (Fig. 10) of the rebar compared to their

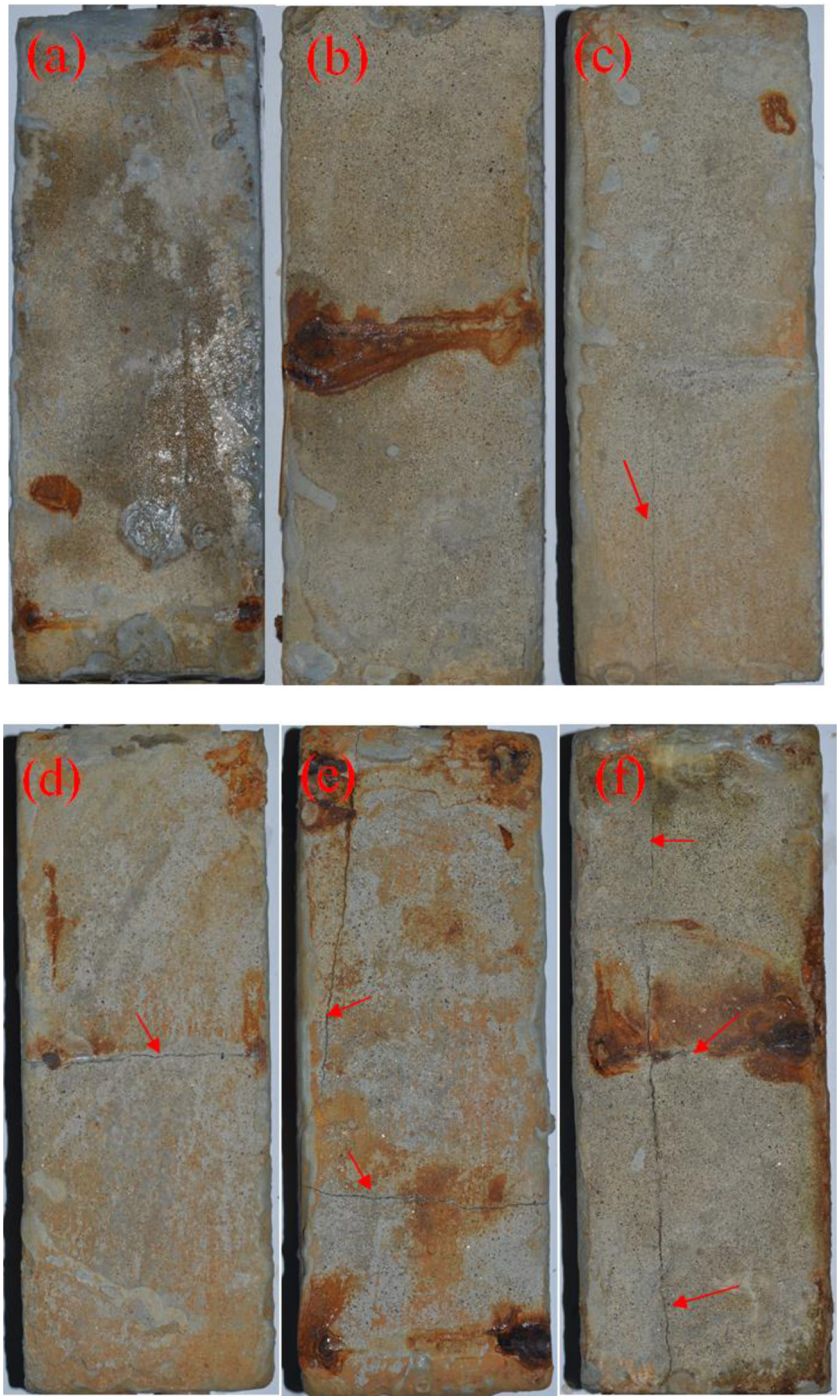

Fig. 9. Photographs of mortar samples that were subjected to tensile and compressive stresses, respectively, of (a) and (b) 12 MPa, (c) and (d) 60 MPa, and (e) and (f) 120 MPa, after being immersed in a 3% NaCl solution for 357 days.

tensile counterparts. This is especially true for the 120 MPa compressive stress that leads to corrosion of almost the entire surface ((Fig. 10 (f)) of the rebar. In contrast, the rebar subjected to tensile stresses is only partly corroded ((Fig. 10 (e)). These results are consistent with those (Figs. 3, 4 and 8) obtained from the electrochemical testing; this re-confirms that compressive stresses result in greater acceleration of the corrosion compared to tensile stresses of the same magnitude.

Aveldaño and Ortega [12] compared the crack behaviour of reinforced concrete beams under compressive and tensile stresses of the same magnitude. The results showed that the corrosion potential of the former is more negative than that of the latter. In addition, the crack in the concrete cover layer on the compressed beam was larger and appeared earlier than that formed in the cover layer subjected to the tensile stress. The gravimetric losses of the rebar in the compressed beam were, however, lower than those in the tensile beam. The trends observed for the electrochemical tests and the crack formation concur with those of previous studies [12]. However, but the results describing the corrosion state (Fig. 10) differ from the gravimetric losses described by Aveldaño and Ortega [12]. This difference may have resulted from error introduced during calculation of the losses, by extrapolating the lengths over which tests were performed in a previous study [12]. In addition, in Aveldaño's study, the stress applied to the rebar is neither purely compressive

Fig. 10. Corrosion state of the rebar under tensile and compressive stresses of (a) and (b) 12 MPa, (c) and (d) 60 MPa, and (e) and (f) 120 MPa, respectively.

nor purely tensile and this may have contributed to the discrepancy between the gravimetric and electrochemical results. The authors attributed the difference in the crack behaviour in the concrete cover layer to the differing Poisson's effect resulting from the action of the tensile and compressive stresses. Furthermore, the failure modes of the concrete/rebar interface under tensile stresses differ from those occurring under compressive stresses, and the aforementioned discrepancy may also be associated with this difference. When the mortar sample undergoes flexural loading, shear stresses act on the compressive side of the rebar/mortar interface. Previous studies [30–32] proposed that the minimum shear stress (τ_{min}) at the rebar/concrete interface (at the supporting point) is obtained from:

$$\tau_{min} = \tau_0 \left(1 - \frac{2e^{\omega L/2}}{1 + e^{\omega L}}\right) \approx \tau_{0\left(1-2e^{-\omega L/2}\right)} \quad (4)$$

where τ_0 is the shear stress of the cross-section at the supporting point and ωL, with values ranging from 5 to 10, is an indicator of the degree of shear connection [31]. In the present study, assuming $\omega L = 6$, τ_{min} of 0.97 MPa and 1.94 MPa are obtained for flexural loading of 2.5 kN and 5.0 kN, respectively. Almusallam [33] reported respective bond strengths of ~0.5 MPa and 1.5 MPa for severely cor-

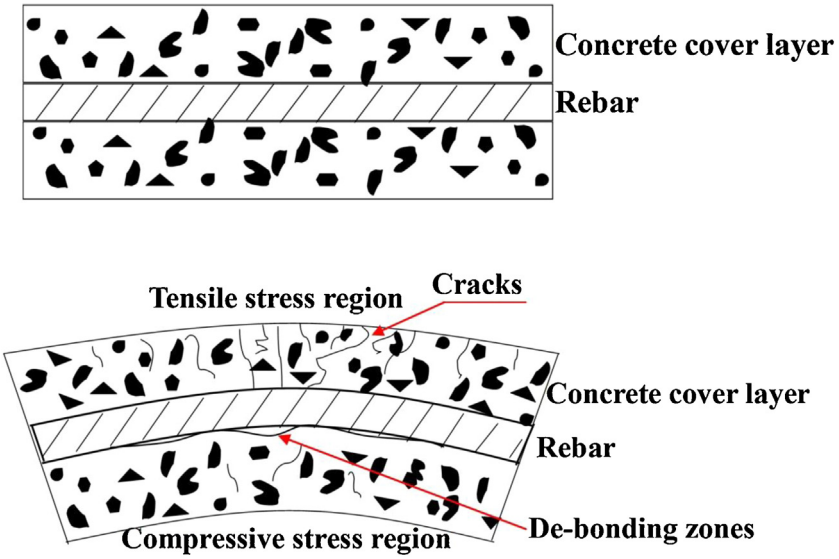

Fig. 11. Schematic showing the degradation of the concrete/steel rebar interface in mortars (a) without an applied stress and (b) subjected to flexural loading.

roded and non-corroded rebar/concrete interfaces. A comparison of these values with the τ_{min} determined in this study, indicates that de-bonding zones will form in the region subjected to compressive stresses. On the tensile side of the mortar, micro-cracks are rapidly formed in the cover layer owing to the low tensile strength of the mortar [34]. Thus, the results in Fig. 8(b) show that the concrete/rebar interface is more severely degraded under compression than that under tension. The schematic in Fig. 11 shows the degradation of the concrete/rebar interface under tensile and compressive stresses. As Fig. 11(a) shows, the rebar is perfectly adhered to the concrete in the non-stressed sample. However, micro-cracks formed along directions perpendicular to the applied tensile stresses [35], in the case of the sample subjected to flexural stresses; de-bonding zones were generated at the concrete/rebar interface (Fig. 11(b)) on the compressed side [10,36]. The corrosion products flow from the concrete/rebar interface into the cracks on the tensile side and fill the de-bonding zones, with progressive corrosion of the rebar. This leads to radial stresses in the concrete on the compressed side [12]. Therefore, the concrete cover layers subjected to compressive stresses crack earlier, and the rebar is more severely corroded, than those subjected to tensile stress of the same magnitude.

4. Conclusions

The corrosion behaviour of the rebar in mortars subjected to flexural stresses is investigated by OCP, LPR, and EIS measurements. After immersed in the 3.0% sodium chloride solution for 357 days, the corrosion state of the rebar in the stressed mortars was examined after removing the mortar cover layers. The following conclusions can be drawn from the results of this study.

1. As the applied stress increases, the OCP, polarization resistance, and impedance of the rebar decrease; the corrosion of the rebar significantly increases.
2. For the same magnitude of stress, the rebar in the compressed mortars have a more negative OCP, and both lower polarization resistance and impedance value than their counterparts that are subjected to tensile stresses; the rebar in the compressed sample is also more severely corroded than that in the tensile sample.
3. The applied stress destroys the concrete/rebar interface and leads to a reduction in the polarization resistance of the rebar. As such, the corrosion of the rebar increases with increasing magnitude of the stress.
4. Modes are introduced to explain the difference between the degradation patterns on the mortar/rebar interface under tensile and compressive stresses. In the case of the sample subjected to flexural stresses, micro-cracks in the mortar formed in the direction perpendicular to the tensile stresses. However, de-bonding zones formed in the mortar/rebar interface subjected to compressive stresses.

Acknowledgements

The authors would like to thank the National Natural Science Foundation of China (51301060), the Fundamental Research Funds for the Central Universities (2015B20814), the Natural Science Research Program for Higher Education in Jiangsu Province, China (No.14KJB430012), and State Key Laboratory of High Performance Civil Engineering Materials (No. 2014CEM003). The project also supported by Key Laboratory of Advanced Civil Engineering Materials (Tongji University), Ministry of Education.

References

[1] L. Hariche, Y. Ballim, M. Bouhicha, S. Kenai, Effects of reinforcement configuration and sustained load on the behaviour of reinforced concrete beams affected by reinforcing steel corrosion, Cem. Concr. Res. 34 (2012) 1202–1209.
[2] N. Anhvu, A. Castel, R. Francois, Effect of stress corrosion cracking on stress–strain response of steel wires used in prestressed concrete beams, Corros. Sci. 51 (2009) 1453–1459.
[3] S.J. Jaffer, C.M. Hansson, Chloride-induced corrosion products of steel in cracked-concrete subjected to different loading conditions, Cem. Concr. Res. 39 (2009) 116–125.
[4] W. Ahn, D.V. Reddy, Galvanostatic testing for the durability of marine concrete under fatigue loading, Cem. Concr. Res. 31 (2001) 343–349.
[5] A. Valiente, Stress corrosion failure of large diameter pressure pipelines of prestressed concrete, Eng. Fail. Anal. 8 (2001) 245–261.
[6] C. Fang, K. Gylltoft, K. Lundgren, M. Plos, Effect of corrosion on bond in reinforced concrete under cyclic loading, Cem. Concr. Res. 36 (2006) 548–555.
[7] E.B. Arteaga, P. Bressolette, A. Chateauneuf, M. Silva, Probabilistic lifetime assessment of RC structures under coupled corrosion–fatigue deterioration processes, Struct. Saf. 31 (2009) 84–96.
[8] C.A. Apostolopoulos, M.P. Papadopoulos, Tensile and low cycle fatigue behavior of corroded reinforcing steel bars S400, Constr. Build. Mater. 21 (2007) 855–864.
[9] J. Blunt, G. Jen, C.P. Ostertag, Enhancing corrosion resistance of reinforced concrete structures with hybrid fiber reinforced concrete, Corros. Sci. 92 (2015) 182–191.
[10] X. Feng, Y. Zuo, Y. Tang, X. Zhao, X. Lu, The degradation of passive film on carbon steel in concrete pore solution under compressive and tensile stresses, Electrochim. Acta 58 (2011) 258–263.
[11] Y. Zhang, Study on corrosion activity of carbon steel in concrete simulated pore solution under static tensile and compressive stresses, M.E., Theses, Clemson University, South Carolina, 2012.
[12] R.R. Aveldaño, N.F. Ortega, Behavior of concrete elements subjected to corrosion in their compressed or tensed reinforcement, Constr. Build. Mater. 38 (2013) 822–828.
[13] G.B. Richard, Advanced Strength and Applied Stress Analysis, McGraw-Hill, New York, 1977.
[14] S.G. Dong, B. Zhao, C.J. Lin, R.G. Du, R.G. Hu, G.X. Zhang, Corrosion behavior of epoxy/zinc duplex coated rebar embedded in concrete in ocean environment, Constr. Build. Mater. 28 (2012) 72–78.
[15] M. Pour-Ghaz, O.B. Isgor, P. Ghods, The effect of temperature on the corrosion of steel in concrete.Part 1: simulated polarization resistance tests and model development, Corros. Sci. 51 (2009) 415–425.
[16] C. Andrade, C. Alonso, J. Gulikers, R. Polder, R. Cigna, O. Vennesland, M. Salta, A. Raharinaivo, B. Elsener, Test methods for on-site corrosion rate measurement of steel reinforcement in concrete by means of the polarization resistance method, Mater. Struct. 37 (2004) 623–643.
[17] C. Cao, M.M.S. Cheung, B.Y.B. Chan, Modelling of interaction between corrosion-induced concrete cover crack and steel corrosion rate, Corros. Sci. 69 (2013) 97–109.
[18] C. Andrade, J.A. Gonzalez, Quantitative measurements of corrosion rate of reinforcing steels embedded in concrete using polarization resistance measurements, Mater. Corros. 29 (1978) 515–519.
[19] H. Yalcyn, M. Ergun, The prediction of corrosion rates of reinforcing steels in concrete, Cem. Concr. Res. 26 (1996) 1593–1599.
[20] M.O.G.P. Bragança, K.F. Portella, M.M. Bonato, C.E.B. Marino, Electrochemical impedance behavior of mortar subjected to a sulfate environment—a comparison with chloride exposure models, Constr. Build. Mater. 68 (2014) 650–658.
[21] A.A. Gürten, K. Kayakırılmaz, M. Erbil, The effect of thiosemicarbazide on corrosion resistance of steel reinforcement in concrete, Constr. Build. Mater. 21 (2007) 669–676.
[22] J.M. Deus, B. Díaz, L. Freire, X.R. Nóvoa, The electrochemical behaviour of steel rebars in concrete: an electrochemical impedance spectroscopy study of the effect of temperature, Electrochim. Acta 131 (2014) 106–115.
[23] W. Morris, A. Vico, M. Vazquez, The performance of a migrating corrosion inhibitor suitable for reinforced concrete, J. Appl. Electrochem. 33 (2003) 1183–1189.
[24] B.J. Pease, M. Geiker, H. Stang, J. Weiss, The design of an instrumented rebar for assessment of corrosion in cracked concrete, Mater. Struct. 44 (2011) 1259–1271.
[25] A. Michel, A.O.S. Solgaard, B.J. Pease, M.R. Geiker, H. Stang, J.F. Olesen, Experimental investigation of the relation between damage at the concrete-steel interface and initiation of reinforcement corrosion in plain and fibre reinforced concrete, Corros. Sci. 77 (2013) 308–321.
[26] C.G. Berrocal, I. Löfgren, K. Lundgren, L. Tang, Corrosion initiation in cracked fibre reinforced concrete: influence of crack width, fibre type and loading conditions, Corros. Sci. 98 (2015) 128–139.
[27] S.J. Jaffer, C.M. Hansson, The influence of cracks on chloride-induced corrosion of steel in ordinary Portland cement and high performance concretes subjected to different loading conditions, Corros. Sci. 50 (2008) 3343–3355.
[28] Y.F. Cheng, J.L. Luo, Electronic structure and pitting susceptibility of passive film on carbon steel, Electrochim. Acta 44 (1999) 2947–2957.

[29] D. Li, R. Zhu, W. Zhang, The acceleration mechanism of stress on anodic dissolution of bare metal surface, Metall. Mater. Trans. A 21 (1990) 3260–3264.
[30] J. Wang, X. Zou, Y. Feng, Bilinear load-deflection model of fiber-reinforced polymer–concrete composite beam with interface slip, Adv. Mech. Eng. 7 (2015) 1–14.
[31] Y. Zou, Z. Zhou, L. Tang, Analysis of flexural stresses and interface shear force of composite beam considering slip effect, Eng. Mech. 11 (2013) 173–179 (in Chinese).
[32] S.T. Smith, J.G. Teng, Interfacial stresses in plated beams, Eng. Struct. 23 (2001) 857–871.
[33] A.A. Almusallam, A.S. Al-Gahtani, A.R. Aziz, Rasheeduzzafart, Effect of reinforcement corrosion on bond strength, Constr. Build. Mater. 10 (1996) 123–129.
[34] A.P. Fantilli, H. Mihashi, P. Vallini, Crack profile in RC, R/FRCC and R/HPFRCC members in tension, Mater. Struct. 40 (2007) 1099–1114.
[35] R. Gao, Q. Li, S. Zhao, Concrete deterioration mechanisms under combined sulfate attack and flexural loading, J. Mater. Civ. Eng. 25 (2012) 39–44.
[36] L.B. Freund, S. Suresh, Thin Film Materials-Stress Defect Formation and Surface Evolution, Cambridge University Press, Cambridge, 2004.